

Heterogeneous & Homogeneous & Bio- & Nano-

CHEMCATCHEM

CATALYSIS

Accepted Article

Title: Enhancement of Mo/ZSM-5 catalysts in methane aromatization by addition of Fe promoters and by reduction/carburization pretreatment

Authors: Sheima Khatib, Apoorva Sridhar, and Mustafizur Rahman

This manuscript has been accepted after peer review and appears as an Accepted Article online prior to editing, proofing, and formal publication of the final Version of Record (VoR). This work is currently citable by using the Digital Object Identifier (DOI) given below. The VoR will be published online in Early View as soon as possible and may be different to this Accepted Article as a result of editing. Readers should obtain the VoR from the journal website shown below when it is published to ensure accuracy of information. The authors are responsible for the content of this Accepted Article.

To be cited as: *ChemCatChem* 10.1002/cctc.201800002

Link to VoR: <http://dx.doi.org/10.1002/cctc.201800002>

Title: Enhancement of Mo/ZSM-5 catalysts in methane aromatization by addition of Fe promoters and by reduction/carburization pretreatment

Author Names and Affiliations: Apoorva Sridhar^a, Mustafizur Rahman^a, Sheima J. Khatib^a

^a Department of Chemical Engineering, Texas Tech University, Lubbock, Texas 79409, United States

Corresponding Author: Sheima J. Khatib, sheima.khatib@ttu.edu

Abstract:

The influence of Fe additive and different types of pretreatment were studied on HZSM-5 supported Mo-oxide (MoO_x) catalysts for methane aromatization. The catalytic behavior of catalysts consisting of 6 wt% Mo/ZSM-5 with 0, 0.2 and 1wt% Fe was tested with two types of pretreatment: 1) heating under He flow, 2) reducing in H_2/CH_4 and carburizing in CH_4 . Under He pretreatment, adding 0.2 wt% Fe improved the benzene yield, but 1 % Fe slightly decreased it. Precarburizing the catalysts resulted in enhanced catalytic properties for all Fe loadings, and furthermore, improved the catalyst stability. The precarburized 6wt% Mo-0.2wt%Fe catalyst presented the highest benzene yield (6.9%), which was almost stable in the subsequent 10-hour test. The fresh and spent catalysts were characterized by XRD, N_2 adsorption, TPR, SEM, TPO and TGA. The results show that precarburized catalysts are more stable due to the formation of smaller amounts of carbon deposits, and consequently lower pore blockage. Addition of Fe causes the carbon deposits to be more reactive and easier to burn off. Higher Fe loadings are linked to the formation of carbon nanotubes.

Introduction

Declining fossil fuel resources and climatic concerns are strong driving forces to switch from non-renewable sources to sustainable processes. Although research is being done extensively to replace the rapidly exhausting non-renewable energy sources with renewable ones, implementation at an industrial scale would take several years. Natural gas, which mostly comprises of methane, is considered the cleanest of the fossil fuels. The high availability and abundance of methane as a major component in natural gas, shale gas, methane hydrates, and also enteric fermentation has instigated the efforts towards converting it to desirable petrochemicals. Therefore, natural gas is an attractive alternative feedstock that is being investigated to fill in the gap between conventional and non-conventional sources of energy. In an era of depletion of natural resources, conversion of methane to desired products is not only an efficient method of utilization of an abundant natural resource, but will also reduce the flaring of greenhouse gases, which ultimately will result in improved quality of living.

Methane conversion into higher hydrocarbons has been extensively studied by researchers in the past decades. Currently, two routes of catalytic conversion of methane are considered: indirect and direct methods. Indirect conversion involves two steps: in the first step, methane is converted into syngas, which comprises mostly of H_2 and CO , by reforming or by partial oxidation. In the second step, syngas is converted into valuable chemicals like gasoline, diesel fuel, paraffins, alkenes, methanol and dimethyl ether (DME) via Fischer-Tropsch process or methanol-to-

hydrocarbons (MTH) catalysis^[1]. Although the indirect route is operated at an industrial scale today, the cost consumption and energy consumption is very high. Whereas direct conversion is a one-step reaction that directly converts methane to added value products. Examples of direct conversion include oxidative coupling of methane (OCM) and dehydroaromatization reaction to aromatics. The major drawback associated with OCM process is the presence of oxygen, which can further oxidize the hydrocarbons to CO₂ and H₂O, thereby decreasing the selectivity of the hydrocarbons at high methane conversions. Although presence of O₂ makes the direct transformation of methane to aromatics thermodynamically favorable, it imposes the same problem as in OCM reactions, where oxidation of methane would take place to form CO₂ and H₂O^{[2][3]}. Since Wang et al.^[4] laid the groundwork on non-oxidative methane dehydroaromatization using Mo-ZSM-5 in 1993, a number of commendable research reports dedicated to this process have been published.

Mo oxides supported on zeolites behave as bi-functional catalysts, where Mo reduces the reactive gas, CH₄, to Mo₂C or Mo_xC_y which is believed to be responsible for the activation of methane and other C₂ intermediates, while oligomerization of ethylene takes place in the Brønsted acid sites located in the ZSM-5 channels, yielding aromatics^{[5][6]}. To overcome the thermodynamic constraints, methane dehydroaromatization reaction should be performed at high temperatures (above 700°C)^[7], however, high reaction temperatures lead to deactivation of the catalyst^{[8][9][10]} due to extensive carbon deposition on the external Brønsted acid sites. Extensive studies have been directed towards improvement of the catalyst stability, including using different zeolite supports like SAPO-34, HY^[11], HMCM-22^{[12][13]}, HZRP-1^[14], and ITQ-2^[15] because of their different pore architectures; modification of the acidity of zeolite^[16]; addition of gases like CO, and CO₂ to the reaction mixture in small quantities which have proven to be useful^{[17][18]}; and doping catalysts with different metals like Zr, W, La, V^[19], Rh, Pt^[20], Cu^[21], Fe^[25], Co^{[22][25]}, Ga, P^[23], Ag, B^[24], Ni^[25], Ir and Pd^[26]. Of these metals, Fe, Co, Ni, Ga, and Ag, have shown the best performance. Attention is mostly directed towards Fe-modified Mo-ZSM-5 catalysts not only because of their stability and promotional effects, but because they are abundant, cheap and environmental friendly, therefore posing potential towards industrial applications^{[27][28]}.

By studying catalysts with different Mo and Fe loadings supported on ZSM-5, Masiero et al.^[29] reported that a new phase Fe₂(MoO₄)₃ was formed as a result of structural interaction of Fe with Mo which was responsible for the improved catalytic properties. Xu et al.^[30] reported that the carbon nanotubes (CNT) induced by presence of Fe helped in accelerating the reaction and increased diffusivity of the products, thereby, enhancing benzene yield. Kubota et al.^[31] studied similar Mo-Fe systems but didn't observe any improvement in the catalytic activity on the addition of Fe. They explained this due to the weakening of the interaction of Mo oxide precursors and acid sites present in ZSM-5 due to competitive consumption of protons in ZSM-5 by the added metal atoms. Aboul-Gheit et al.^[25] observed low catalytic activity when Mo-ZSM-5 was modified with group VII metals (Fe, Zn, Co) and ascribed it to the influence of these metals on the electronic properties of Mo. Sun et al. reported that the presence of Fe promoted the formation of carbon nanotubes which are responsible for the enhanced catalytic stability and higher benzene yields^[28]. Until now, no definitive conclusion has been established regarding the effect of Fe additive on Mo catalysts.

Pretreatment is also known to play a key role in improving the catalytic performance. Tempelman et al. [32] and Tan [33] have reported that precarburization of the catalysts seems to improve their performance in comparison to He pretreatment, as precarburization results in conversion of the Mo oxides to Mo carbides, which are believed to be the active sites that convert methane to C₂ species. However, to the best of our knowledge, precarburization of Mo catalysts modified with a second metal has not been investigated.

In the current study, we aim to investigate the promotional effects of Fe on Mo oxides supported in HZSM-5 zeolite, in the direct conversion of methane to aromatics under non-oxidative conditions under two different pretreatment conditions: under He flow and under CH₄/H₂ flow. We will refer to the latter as “precarburization”.

Results

Activity data

Figure 1 represents the yield of benzene as a function of time on stream (TOS) over the catalysts 6Mo/ZSM-5, 6Mo-0.2Fe/ZSM-5 and 6Mo-1Fe/ZSM-5 undergoing two different pretreatments: 1) heating under He flow (open symbols) and 2) reduction in diluted CH₄/H₂ followed by carburization in pure CH₄. The general trend for all catalysts, regardless of the pretreatment method employed, is an initial increase in yield to benzene within the first 100 mins of reaction (induction period), followed by a drop over a longer period of reaction time. However, a clear difference in the behavior of the catalysts with the different pretreatment methods is observed: the catalysts that undergo precarburization (reduction + carburization pretreatment) present higher yields to benzene with TOS. Furthermore, the drop they show in benzene yield over time is less pronounced compared to the He pretreated catalysts. The catalyst with the best behavior is 6Mo-0.2Fe/ZSM-5, which presents not only the highest benzene yield, but also is the most stable, with no drop in benzene yield after 600 mins of TOS. Table 1 compares the % decrease in the benzene yield for the catalysts undergoing the two different pretreatments after 600 mins of reaction. It is observed that the % decrease in benzene yield is lower for catalysts that undergo precarburization irrespective of the type of metal loading. For both types of pretreatment, adding Fe improves the catalytic stability, since the % decrease for both 0.2 wt% and 1 wt% Fe catalysts is lower than the catalyst with only Mo (6Mo/ZSM-5). The % decrease in benzene yield follows the trend 6 Mo/ZSM-5 > 6Mo-1Fe/ZSM-5 > 6Mo-0.2Fe/ZSM-5 for both types of pretreatment.

Table 1. Comparison of % decrease in benzene yield when the catalysts undergo the two types of pretreatment

Catalyst	% Decrease in benzene yield (He pretreatment)	% Decrease in benzene yield (CH ₄ /H ₂ pretreatment)
6 Mo-ZSM-5	38.0%	11.0%
6 Mo-0.2 Fe-ZSM-5	16.1%	0.6%
6 Mo-1-Fe-ZSM-5	31.0%	7.7%

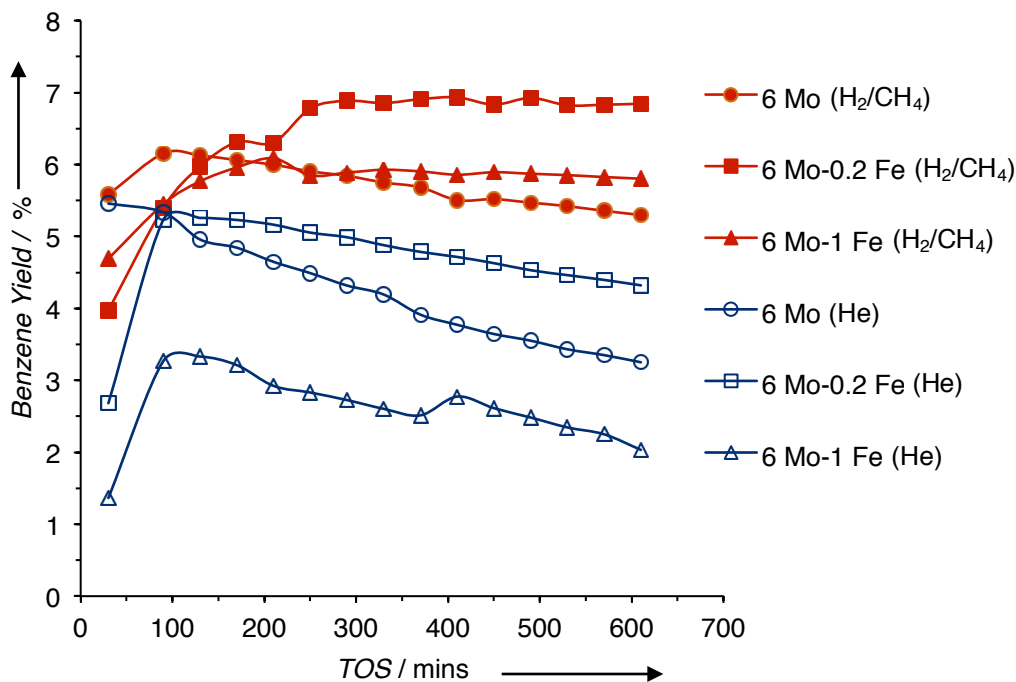


Figure 1. Benzene yield for catalysts 6Mo/ZSM-5, 6Mo-0.2Fe/ZSM-5, and 6Mo-1Fe/ZSM-5. Open symbols correspond to He-pretreated catalysts and closed symbols correspond to precarburized catalysts.

Although adding Fe improves the stability, there is a compromise: better stability is obtained in catalysts with lower loading of Fe (0.2wt%Fe versus 1 wt% Fe). As observed in Figure 1, in the case of the He pretreated catalysts, adding 0.2wt% Fe to the 6Mo/ZSM-5 catalyst improves the benzene yield, however, when the amount of Fe is increased to 1wt%, the catalyst presents lower yields to benzene. In the precarburized catalysts, the presence of both 0.2wt% and 1wt% Fe improves benzene yields with respect to 6Mo/ZSM-5, however, the smaller loading of Fe, 0.2 wt%, results in a higher benzene yield compared to 1 wt%. From these results, we can conclude that adding an optimum amount of Fe can improve catalytic performance, regardless of the kind of pretreatment employed.

The evolution of ethylene yield with TOS for both He pretreated and precarburized catalysts is represented in Figure 2. It is observed that contrary to what happens with benzene yield, the yield of ethylene continues increasing over long periods of reaction time. The ethylene yield increases in the order 6 Mo-0.2Fe/ZSM-5 < 6 Mo-1Fe/ZSM-5 < 6Mo/ZSM-5, which is the opposite to the trend obtained with benzene yield in the case of the precarburized catalysts. This phenomenon has been observed previously in literature^[32] and has been attributed to the gradual blocking of the zeolite channels by coke deposits on surface Brønsted acid sites. As reaction proceeds, carbon deposits cover the Brønsted acid sites and reduce the zeolite pore diameters, therefore methane is activated and converts to C₂ species, such as ethylene, which cannot polymerize to bigger species due to channel constraints. Over time this results in higher ethylene yields at the expense of benzene formation.

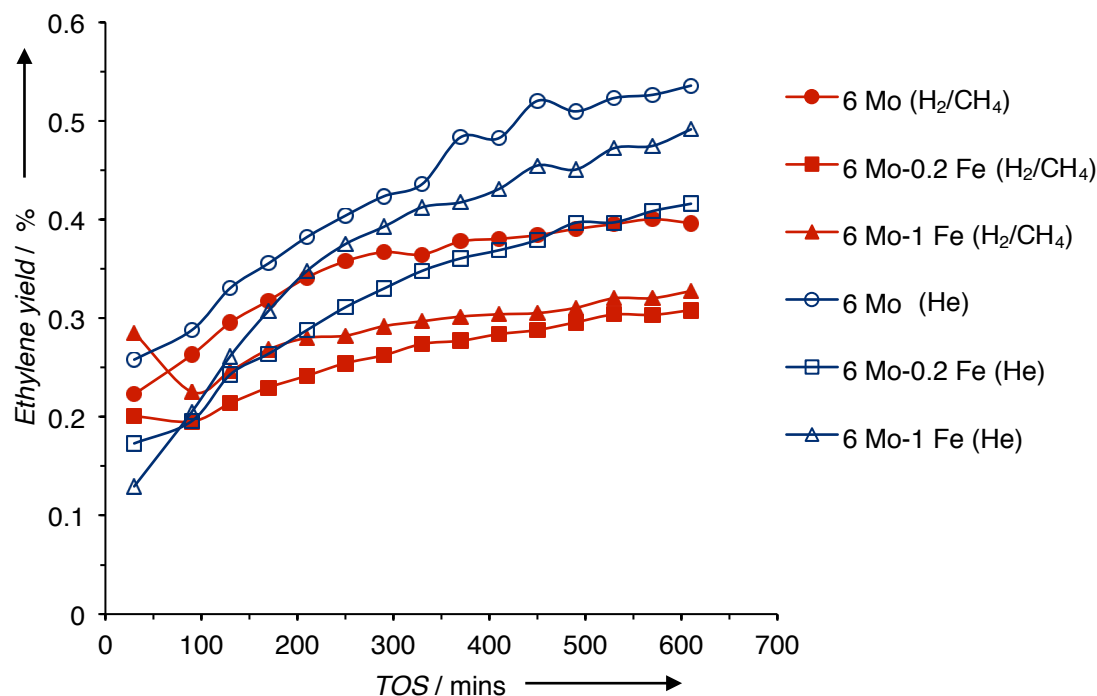


Figure 2. Ethylene yield of He-pretreated and precarburized catalysts: 6Mo/ZSM-5, 6Mo-0.2Fe/ZSM-5, and 6Mo-1Fe/ZSM-5.

Methane conversion with respect to the benzene selectivity of the catalysts is represented in Figure 3. This type of figure compares the specificity of the active sites for the different catalysts and can serve to determine the influence of 1) the presence of Fe on the Mo catalysts and 2) the type of pretreatment on the catalytic behavior. Various important points are observed in the figure. On one hand, when comparing catalysts with the same metal loadings and different pretreatments, we observe that generally higher conversions and selectivities are obtained for the cases of 6Mo-0.2Fe/ZSM-5 and 6Mo-1Fe/ZSM-5, when going from He pretreatment to precarburization. In the absence of Fe, for 6Mo/ZSM-5, the selectivity does not vary, but higher CH₄ conversions are obtained when changing from He pretreatment to precarburization. On the other hand, when comparing catalysts with different metal loadings that have undergone the same type of pretreatment, we observe that for a specific CH₄ conversion (dashed lines in Figure 3) the different catalysts present different benzene selectivities, indicating that the active sites are of a different nature depending on the amount of Fe that is incorporated into the Mo catalyst. In the case of the He pretreated samples, represented with blue, open symbols, for similar values of conversion, the selectivity to benzene increases in the order 6 Mo-1Fe/ZSM-5 < 6 Mo/ZSM-5 < 6Mo-0.2Fe/ZSM-5, whereas for the precarburized catalysts, at a certain CH₄ conversion, benzene selectivity increases in the order 6 Mo/ZSM-5 < 6 Mo-1Fe/ZSM-5 < 6Mo-0.2Fe/ZSM-5.

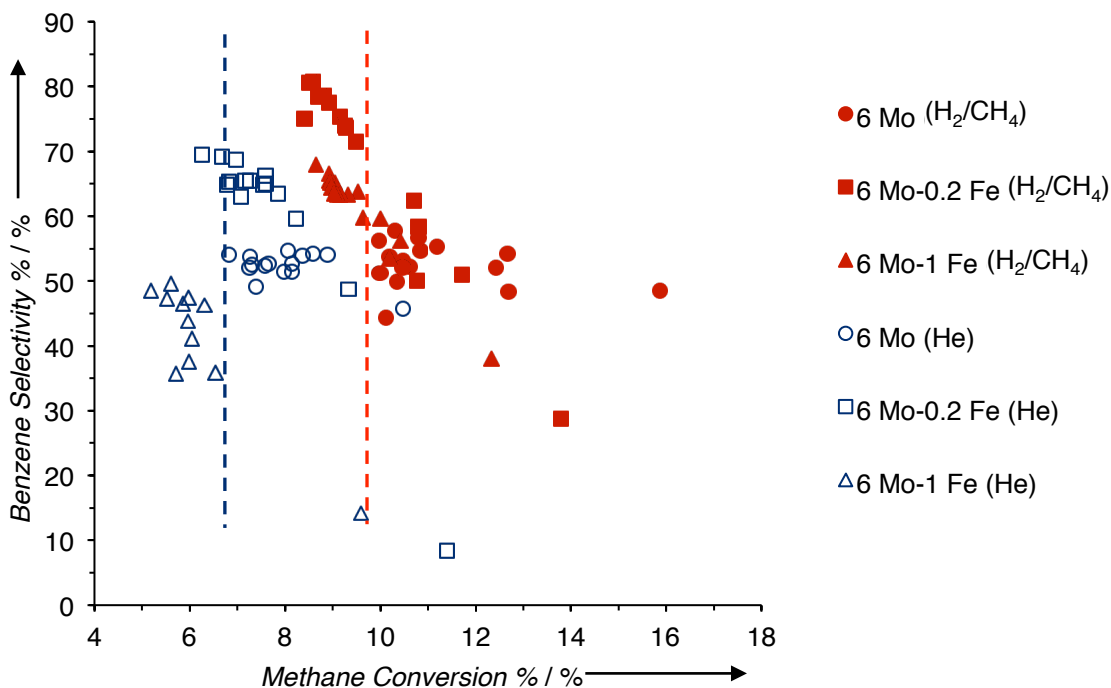


Figure 3. Methane conversion vs benzene selectivity plot for He-pretreated and precarburized catalysts: 6Mo/ZSM-5, 6Mo-0.2Fe/ZSM-5, and 6Mo-1Fe/ZSM-5. Open symbols correspond to He-pretreated catalysts and closed symbols correspond to precarburized catalysts.

N₂ Isotherms and BET Surface areas

BET surface area of both fresh and spent catalysts was measured to determine the change in surface area of the catalysts after reaction. The adsorption and desorption isotherms of the fresh and spent precarburized catalysts are displayed in Figure 4. All the catalysts exhibit Type IV isotherms, indicating presence of micropores with some mesopores. From the isotherms, we also observe that the nitrogen uptake by the fresh catalysts is greater than the spent catalysts, probably due to pore blocking by coke deposition in the latter. Table 2 summarizes the BET surface area of the fresh and spent catalysts. For both types of pretreatment, the surface area of the spent catalysts decreases with respect to the fresh ones, although the decrease in surface area is more drastic for the He-pretreated catalysts, explaining thus their lower stability with TOS. The addition of Fe in the fresh catalyst does not seem to influence the surface area much. The % decrease in surface area from fresh to spent catalysts is indicated in brackets in Table 2. For the precarburized catalysts, the highest % decrease is observed in 6Mo/ZSM-5, followed by 6Mo-1Fe/ZSM-5 and 6Mo-0.2Fe/ZSM-5, which is in line with the trend observed in % decrease in benzene yield.

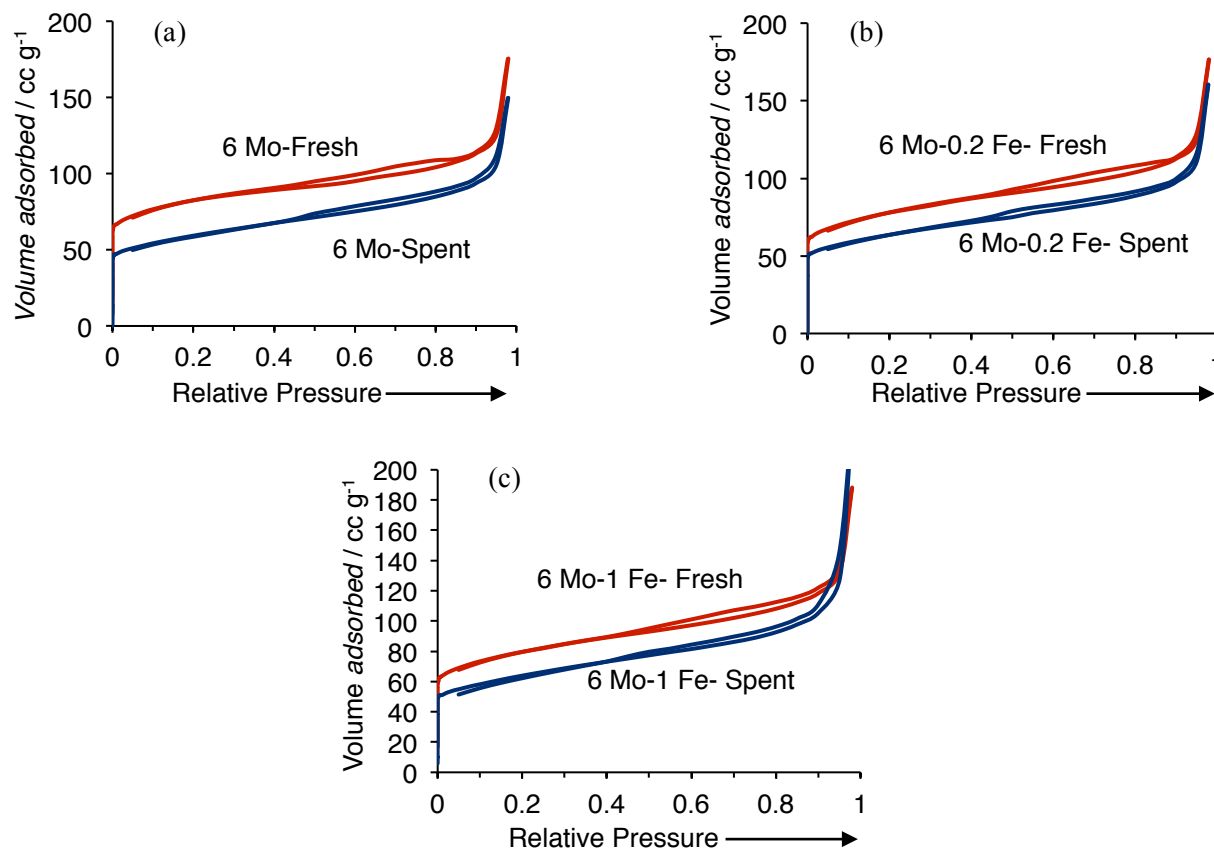


Figure 4. Adsorption and desorption isotherms of Fresh and Spent catalysts (a) 6Mo/ZSM-5 (b) 6Mo-0.2Fe/ZSM-5 (c) 6Mo-1Fe/ZSM-5. (The spent catalysts underwent reaction at 700°C under 91% CH₄/N₂ with a space velocity of 1500 ml/g·hr for 10 hours.)

Table 2. BET Surface areas of the fresh and spent catalysts. The numbers in brackets represent the % decrease in surface area from fresh to spent samples. (The spent catalysts underwent reaction at 700°C under 91% CH₄/N₂ with a space velocity of 1500 ml/g·hr for 10 hours.)

Catalyst	BET surface area of He-pretreated catalysts (m ² /g)	BET surface area of precarburized catalysts (m ² /g)
6 Mo -ZSM-5 - Fresh	283	298
6 Mo -0.2 Fe-ZSM-5- Fresh	290	268

6 Mo -1 Fe-ZSM-5- Fresh	292	285
6 Mo -ZSM-5- Spent	150 (47%)	211 (29%)
6 Mo -0.2 Fe-ZSM-5- Spent	158 (46%)	230 (14%)
6 Mo -1 Fe-ZSM-5- Spent	143 (51%)	227 (20%)

X-Ray Diffraction

The XRD patterns of the fresh and spent 6Mo/ZSM-5, 6Mo-0.2Fe/ZSM-5, 6Mo-1Fe/ZSM-5 catalysts and calcined ZSM-5 support are represented in Figures 5, 6 and 7. All catalysts exhibit the diffraction peaks corresponding to ZSM-5 (Figure 5), implying that the catalyst support suffered no major structural changes after Mo and Fe were incorporated in the structure. The crystallinity of the ZSM-5 support is preserved even after the catalysts have been under reaction conditions for over 10 hours. It has been established that the two peaks located between $2\theta = 5-10^\circ$ are sensitive to the presence of any species in the micropore channel structure of the zeolite^[34]. We see that the intensity of these peaks in the fresh catalysts decreases in comparison to the parent H-ZSM-5. This decrease in intensity suggests good dispersion of Mo and Fe species into the zeolite channels^{[29][34]}. No changes are observed in the diffraction patterns of the spent samples. Figure 6 presents a close-up of the XRD patterns in the $2\theta = 25-29^\circ$ region, in order to better discern the peaks corresponding to Mo oxide species. In the case of the He-pretreated catalysts, a peak at $2\theta = 27.3^\circ$ assigned to crystalline MoO₃ (JCPDS File No. 05-05058) is detected for 6Mo/ZSM-5, the zeolite support also presents a weak peak at this angle, however it's intensity is much larger in the 6Mo/ZSM-5 catalyst compared to the bare H-ZSM-5. The MoO₃ peak becomes less intense again in the catalysts that have Fe incorporated, 6Mo-0.2Fe/ZSM-5 and 6Mo-1Fe/ZSM-5, which indicates that the presence of Fe results in a Mo-Fe interaction that decreases the crystallinity of the MoO₃ species present in the fresh catalysts. Figure 7 shows a close-up of the diffraction patterns of the precarburized catalysts in the $2\theta = 39-47^\circ$ region; a weak broad peak at $2\theta = 39.5^\circ$ appears for fresh and spent 6Mo-1Fe/ZSM-5, which has been assigned to crystalline Mo₂C (JCPDS File No. 35-0787).

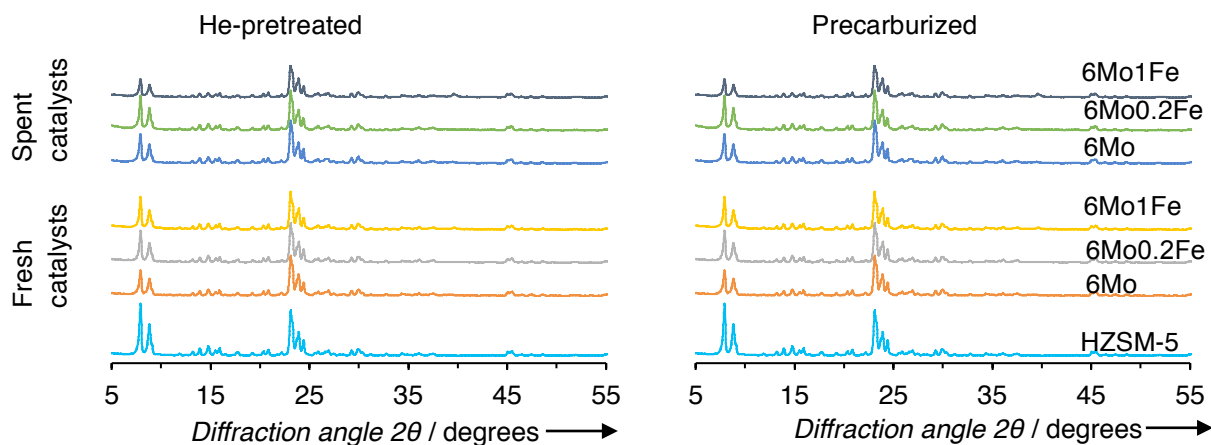


Figure 5. XRD patterns of calcined ZSM-5 support, fresh and spent catalysts 6Mo/ZSM-5, 6Mo-0.2Fe/ZSM-5, and 6Mo-1Fe/ZSM-5, in the range $2\theta = 5^\circ$ - 60° . (The spent catalysts underwent reaction at 700°C under 91% CH_4/N_2 with a space velocity of $1500 \text{ ml/g}\cdot\text{hr}$ for 10 hours.)

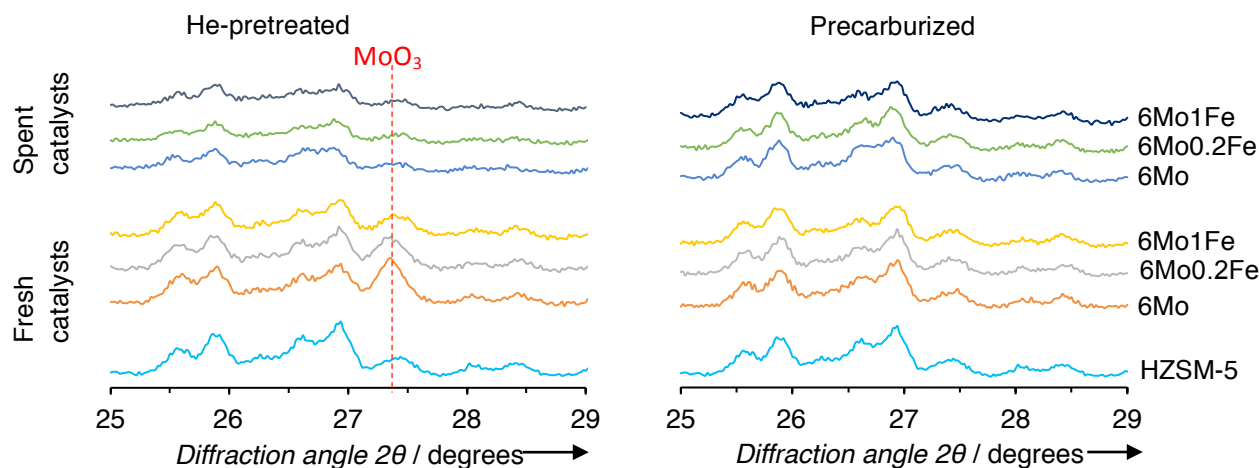


Figure 6. XRD patterns of calcined ZSM-5, fresh and spent catalysts 6Mo/ZSM-5, 6Mo-0.2Fe/ZSM-5, and 6Mo-1Fe/ZSM-5, in the range $2\theta = 25^\circ$ - 29° . (The spent catalysts underwent reaction at 700°C under 91% CH_4/N_2 with a space velocity of $1500 \text{ ml/g}\cdot\text{hr}$ for 10 hours.)

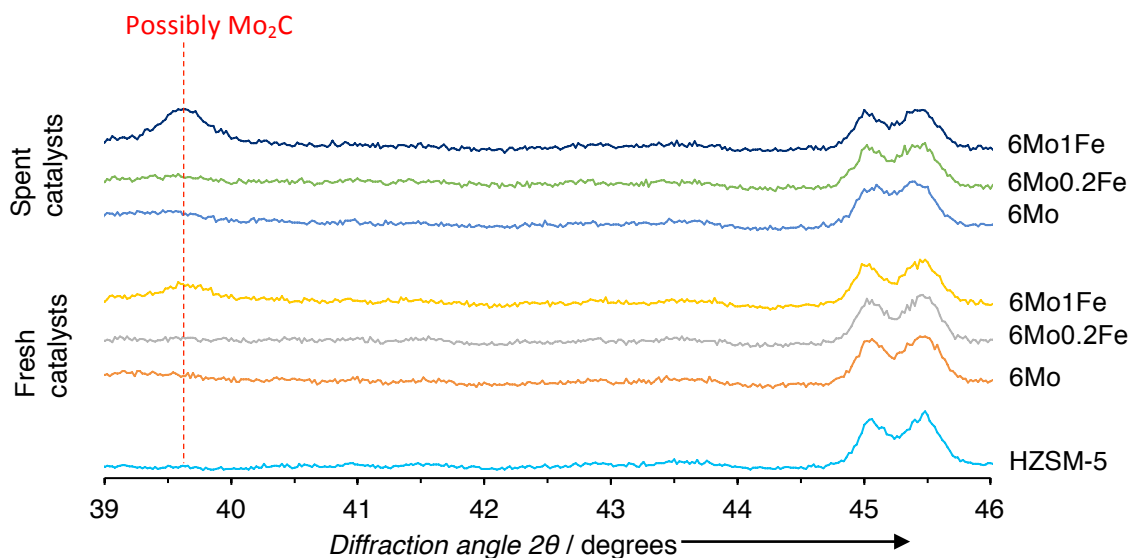


Figure 7. XRD patterns of precarburized fresh and spent catalysts 6Mo/ZSM-5, 6Mo 0.2Fe/ZSM-5, and 6Mo-1Fe/ZSM-5, in the range $2\theta = 39^\circ$ - 47° . (The spent catalysts underwent reaction at 700°C under 91% CH_4/N_2 with a space velocity of $1500 \text{ ml/g}\cdot\text{hr}$ for 10 hours.)

Temperature Programmed Reduction

Temperature programmed reduction (TPR) studies help us understand the degree of reducibility of the metal phases in the catalysts. Figure 8 represents the H_2 -TPR data for fresh 6Mo/ZSM-5, 6Mo-0.2Fe/ZSM-5 and 6Mo-1Fe/ZSM-5 catalysts before pretreatment. All the catalysts show a similar trend, with two reduction peaks around 580 and 770°C which have been attributed to the reduction of MoO_3 species to MoO_2 ($\text{Mo}^{6+} \rightarrow \text{Mo}^{4+}$) and MoO_2 to Mo metal ($\text{Mo}^{4+} \rightarrow \text{Mo}^0$), respectively [35][36][37]. A slight shift to lower temperature is observed for the first peak as Fe content increases, which is in line with previous work where the presence of nano Fe structures on Mo-based catalysts was found to enhance the Mo oxide reducibility [28]. The high temperature peak does not shift in the case of 6Mo/ZSM-5 and 6Mo-0.2Fe/ZSM-5, however with higher Fe content, the peak becomes broader, slightly shifts to higher temperature and a new shoulder appears around 850°C . TPR measurements of Fe oxides result in reduction peaks at temperatures in the range of 400 - 550°C [38], but reduction peaks at these temperatures are not detected, which is consistent with the small amounts of Fe species that are present in the catalysts.

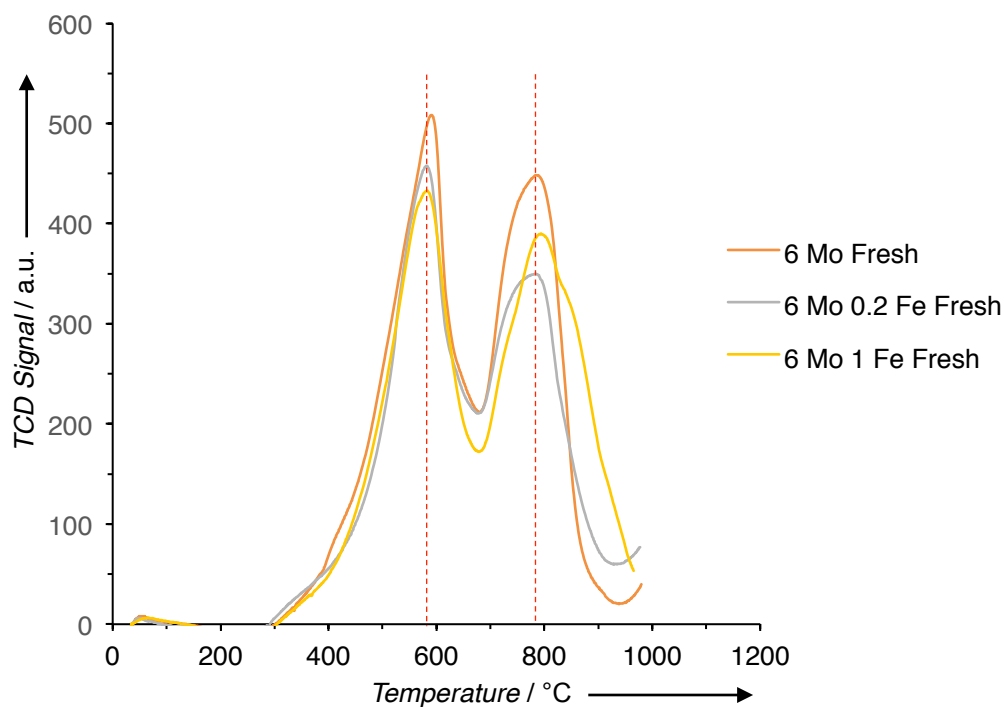
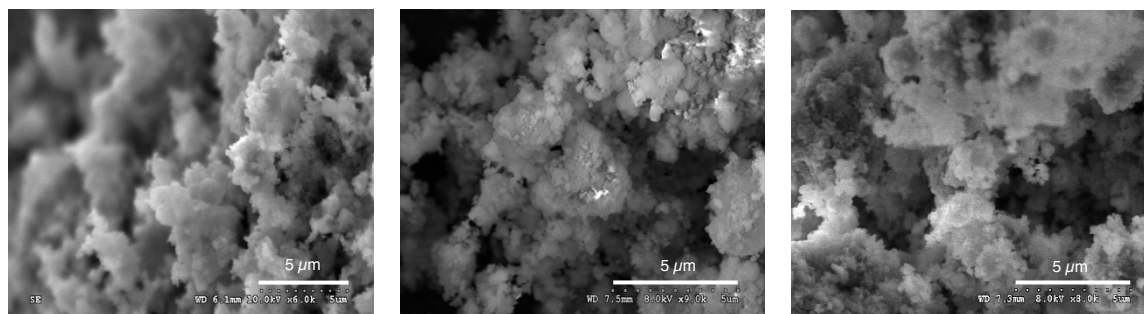


Figure 8. TPR of fresh (catalysts before pretreatment) 6Mo/ZSM-5, 6Mo-0.2Fe/ZSM-5, catalysts and 6Mo-1Fe/ZSM-5 catalysts.

Scanning electron microscopy

SEM imaging was performed in order to investigate the morphology of the catalysts. Figures 9 and 10 represent the SEM images of the fresh and spent catalysts 6Mo/ZSM-5, 6Mo-0.2Fe/ZSM-5 and 6Mo-1Fe/ZSM-5, with He pretreatment and precarburization respectively. All the fresh catalysts look alike, and no morphological changes are observed regardless of the type of pretreatment or type of metal loading. Only in the case of the fresh precarburized 6Mo-1Fe/ZSM-5 catalyst some carbon nanotubes are observed. The scenario changes in the spent catalysts. The spent pretreated catalysts show formation of carbon nanotubes in both the catalysts that contain Fe, 6Mo-0.2Fe/ZSM-5 and 6Mo-1Fe/ZSM-5 (Figures 9 (e) and (f)), however, in the spent precarburized catalysts, carbon nanotubes are only observed for the catalyst with higher Fe loading, 6Mo-1Fe/ZSM-5 (Figure 10 (f)).



(a)

(b)

(c)

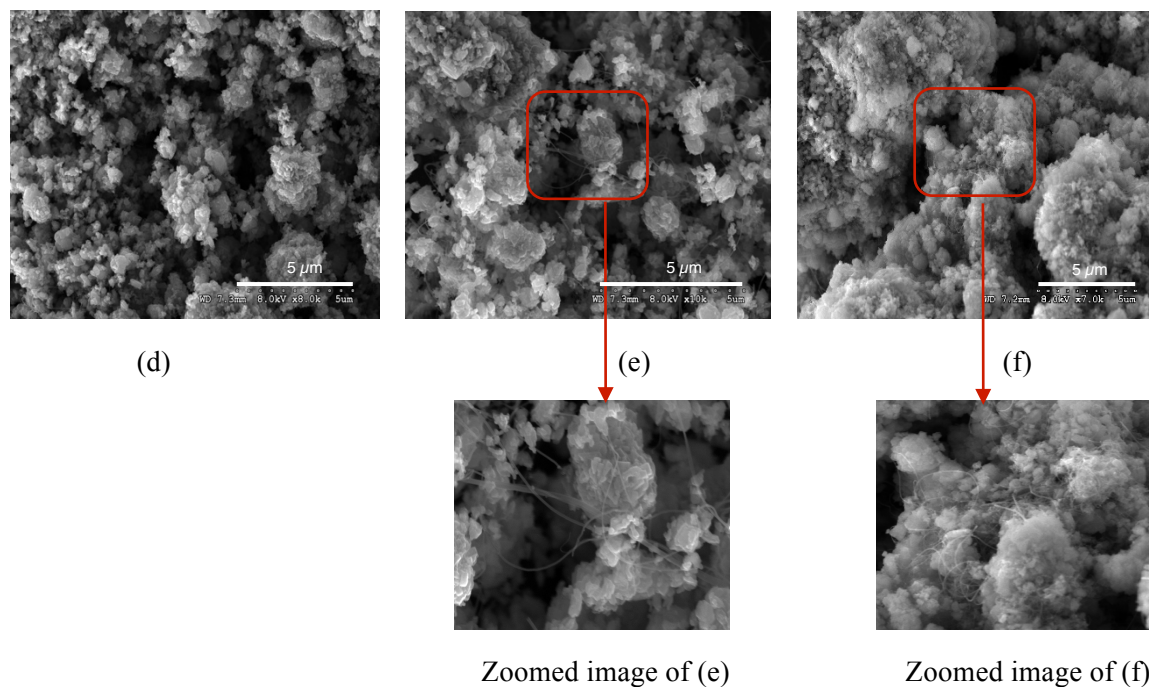


Figure 9. SEM images of the fresh oxide catalysts (a) 6Mo/ZSM-5 (b) 6Mo-0.2Fe/ZSM-5 (c) Mo-1Fe/ZSM-5 and of the spent oxide catalysts (d) 6Mo/ZSM-5 (e) 6Mo-0.2Fe/ZSM-5 (f) Mo-1Fe/ZSM-5. (The spent catalysts underwent reaction at 700°C under 91% CH₄/N₂ with a space velocity of 1500 ml/g·hr for 10 hours.)

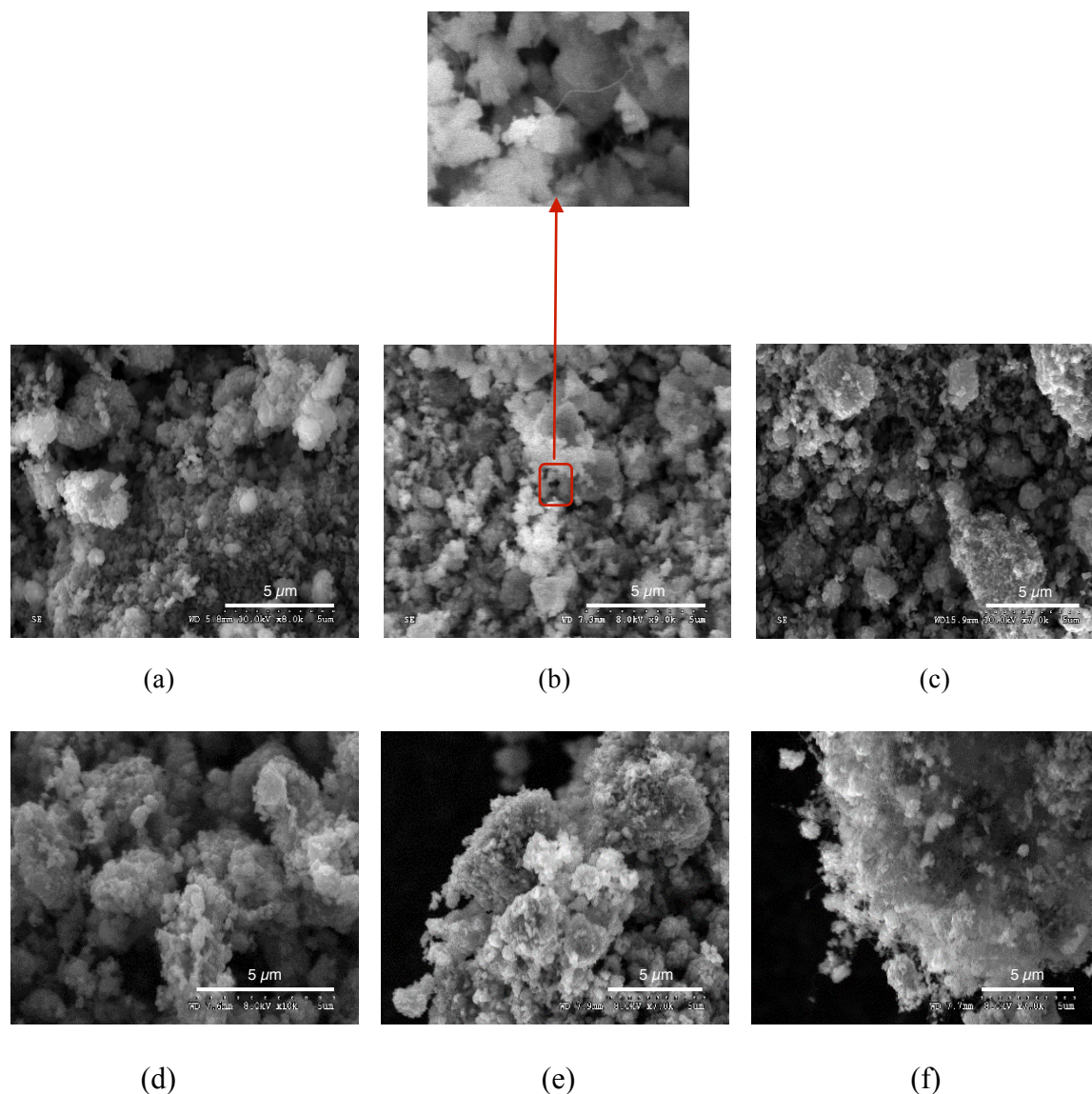


Figure 10. SEM images of the fresh carbide catalysts (a) 6Mo/ZSM-5 (b) 6Mo-1Fe/ZSM-5 (c) Mo-0.2 Fe/ZSM-5 and of the spent carbide catalysts (d) 6Mo/ZSM-5 (e) 6Mo-0.2Fe/ZSM-5 (f) Mo-1Fe/ZSM-5. (The spent catalysts underwent reaction at 700°C under 91% CH₄/N₂ with a space velocity of 1500 ml/g·hr for 10 hours.)

Thermogravimetric Analysis

TGA technique was implemented to quantify the amount of carbon present in the precarburized catalysts before and after reaction. Figure 11 represents the TGA and DTG profiles obtained for fresh and spent catalysts, 6Mo/ZSM-5, Mo-0.2Fe/ZSM-5, and 6Mo-1Fe/ZSM-5. It can be observed that the weight loss is more prominent in the spent catalysts than in the fresh catalysts, due to the formation of carbon deposits during reaction. The peaks in the DTG profiles (Figure 11 (c), (d)) reflect the weight losses observed in the TGA profiles (Figure 11 (a), (b)). The DTG

peaks that appear in the 25-300°C temperature range correspond to weight loss due to evaporation of water^[39], and the peaks that appear between 400-700°C correspond to weight loss due to burning off of carbon deposits^[40]. It is important to note that even the fresh catalysts contain a small amount of carbon deposits, formed during the precarburization treatment. The weight gain observed in the 300-400°C range, in both fresh and spent catalysts, is attributed to the formation of Mo oxide by oxidation of Mo carbide species, since MoO₃ has a higher molecular weight than Mo₂C in Mo/ZSM-5^[41]. In the present study, two of the catalysts contain Fe, and although it is not detected by XRD, the existence of Fe carbide species is probable, therefore the weight gain observed in the 300-400°C range may be due to a combination of the oxidation of both Mo and Fe carbide species. Since the different Mo and Fe carbide phases have not been detected or quantified by the characterization techniques employed, the amount of carbon originating from carbide species cannot be calculated here. We will however assume that the carbon that is burnt off at higher temperature originates only from carbon deposits. In the case of the fresh catalysts, the carbon deposits are formed due to the precarburization treatment, while for spent catalysts the carbon burnt off results from the carbon deposits formed during precarburization and during reaction.

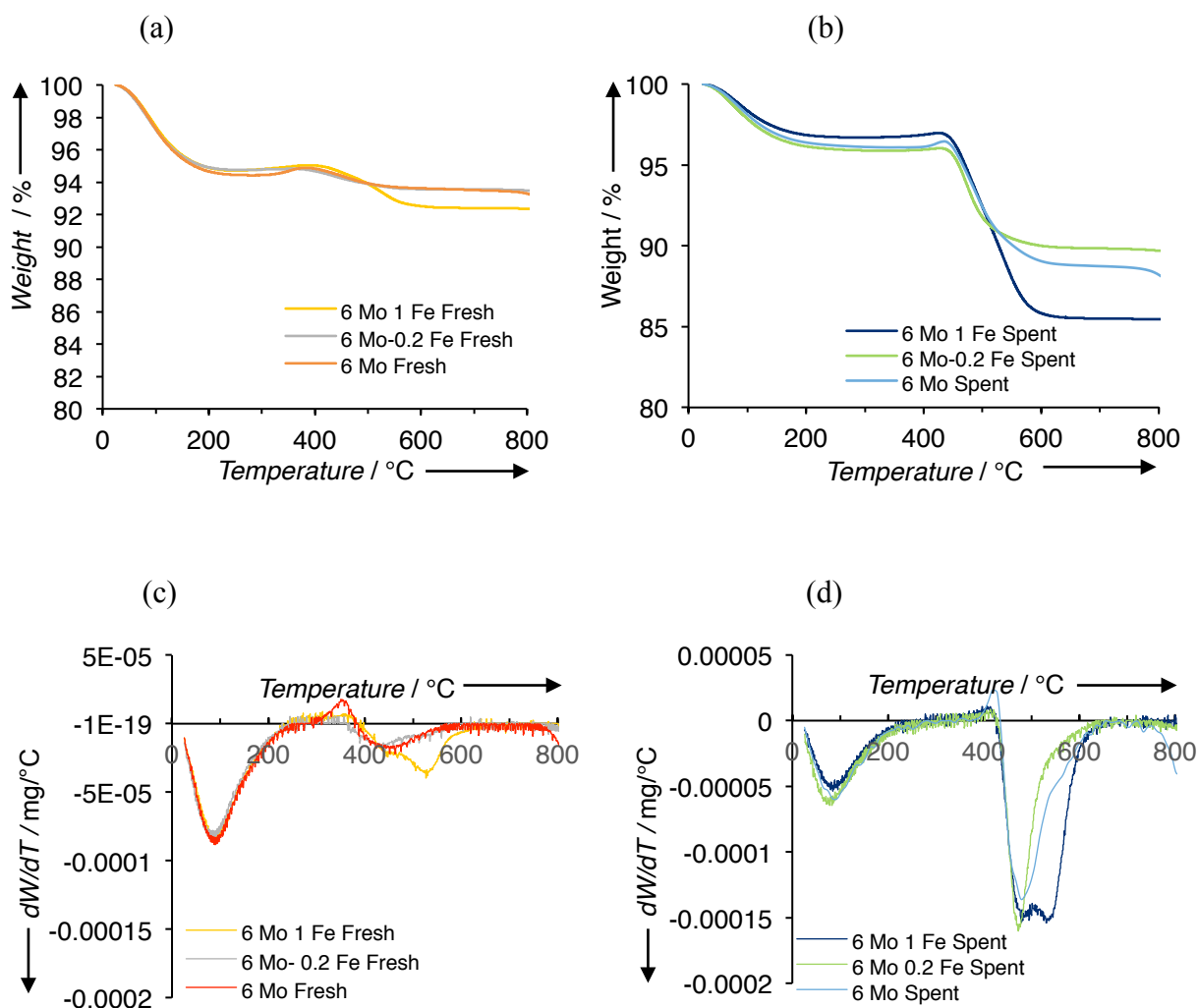


Figure 11. (a) TGA data of all the fresh precarburized catalysts (b) TGA data of all the spent precarburized catalysts (c) DTG data of all the fresh precarburized catalysts (d) DTG data of all the spent precarburized catalysts. (The spent catalysts underwent reaction at 700°C under 91% CH₄/N₂ with a space velocity of 1500 ml/g·hr for 10 hours.)

The total amounts of carbon deposits burnt off were calculated from the TGA profiles (calculation details explained in the Experimental section) and are listed in Table 3. The total amount of carbon deposits formed in reaction is calculated by subtracting the amount of carbon deposits in the fresh, precarburized catalysts from the total amount measured in the spent catalysts. The amount of coke formation decreases in the order 6Mo-1Fe/ZSM-5 > 6Mo/ZSM-5 > 6Mo-0.2Fe/ZSM-5 in both fresh and spent catalysts, showing that a higher content in Fe results in formation of higher amounts of carbon deposits, however the optimum amount of Fe, 0.2 wt% results in a smaller amount of carbon deposition.

Table 3. Amount of coke burnt off from the fresh and spent precarburized catalysts. (The spent catalysts underwent reaction at 700°C under 91% CH₄/N₂ with a space velocity of 1500 ml/g·hr for 10 hours.)

Catalyst	Amount of coke burnt off (mg/g catalyst) from fresh catalyst	Amount of coke burnt off (mg/g catalyst) from spent catalyst	Amount of coke deposited during reaction (mg/g catalyst)
6 Mo	14.5	83.8	69.3
6 Mo 0.2 Fe	13.2	68.8	55.6
6 Mo 1 Fe	27.9	134.2	106.3

Temperature Programmed Oxidation

TPO was performed on the spent catalysts to gain insight on the type of carbon that is deposited on the catalysts by monitoring the evolution of CO_x and H₂O burning off the catalysts. The TPO-TCD profiles are represented in Figures 12 and 13. From Figure 12 it is observed that the TPO profile for He-pretreated 6Mo/ZSM-5 presents a peak at 542 °C and a shoulder at 570 °C; 6Mo-0.2Fe/ZSM-5 presents similar peaks, but the shoulder at 568 °C is less intense; the profile for 6Mo-1Fe/ZSM-5 is slightly different, with a shoulder at 504 °C and a peak at 557 °C. Other groups have obtained similar TPO profiles studying spent zeolite-supported Mo oxides in CH₄ aromatization^{[13][30][42][43]}, and have attributed peaks between 490°C and 520°C to the oxidation of “soft coke”, mainly associated with the carbonaceous deposits that are associated with the Mo species, while the high-temperature shoulder observed for 6Mo/ZSM-5 at around 570°C has been assigned to “hard” coke formation, associated with the carbon deposited on the Brønsted acid

sites within the zeolite pores. In the case of 6Mo-1Fe/ZSM-5, the high temperature peak (at 557°C) is more intense than the low temperature peak, which only appears as a shoulder, coinciding with the fact that this catalyst presents higher formation of carbon nanotubes, as observed in its SEM image (Figure 11 (f)). Since the carbon nanotubes are highly crystalline in nature, it is reasonable to assume that they burn off in the high temperature region, which is consistent with results obtained by Xu et al. who observed an increase in the intensity of the high temperature peak with increasing C nanotube formation as Fe content increased^[30]. Both low and high temperature peaks shift to lower temperatures as Fe content increases from 0 to 0.2 to 1 wt% Fe: 542 °C → 532 °C → 504 °C, and 570°C → 568 °C → 557 °C respectively, indicating that the presence of Fe results in the formation of more reactive carbon deposits that are easier to burn off.

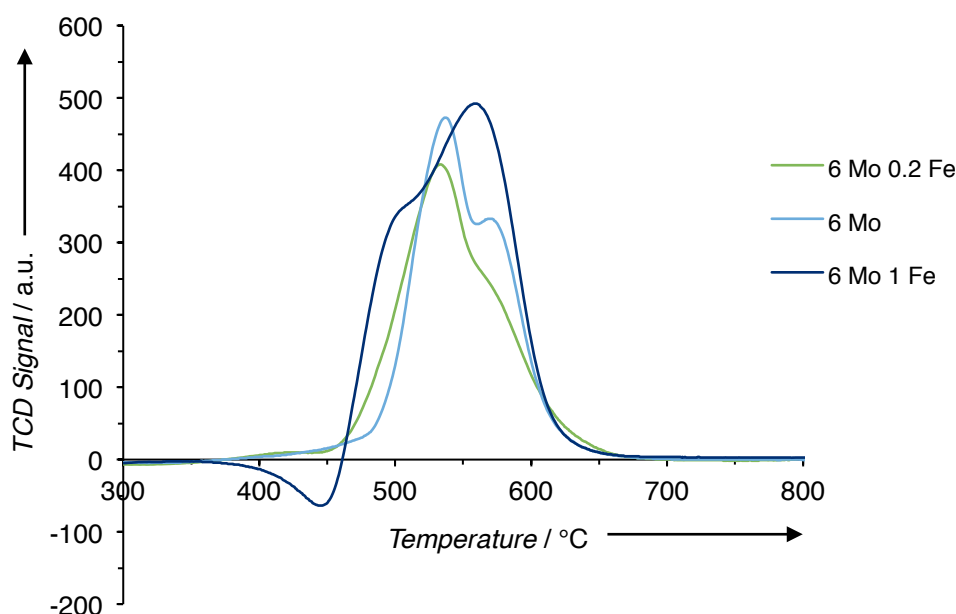


Figure 12. TPO of spent He-pretreated catalysts 6Mo/ZSM-5, 6Mo-0.2 Fe/ZSM-5 and 6Mo-1Fe/ZSM-5. (The spent catalysts underwent reaction at 700°C under 91% CH₄/N₂ with a space velocity of 1500 ml/g·hr for 10 hours.)

Figure 13 represents the TPO of the fresh and spent, precarburized catalysts. It is observed that precarburizing the catalysts results in even more reactive coke deposits after reaction. Here the TPO profiles of the spent catalysts are very similar to the ones obtained for the He-pretreated spent catalysts, however two differences are observed: 1) the low temperature peaks are shifted to lower temperatures by around 40°C for 6Mo/ZSM-5 and 6Mo-0.2Fe/ZSM-5; 2) the high temperature peaks are not shifted but their intensities are lower compared to the He-pretreated samples in Figure 12. These differences mean that precarburizing the catalysts results in more reactive Mo-associated carbon deposits and in lower formation of hard coke. There is an exception in the case of 6Mo-1Fe/ZSM-5, where the contribution to the high temperature peak does not seem to vary regardless of the pretreatment, as observed when comparing the TPO

profiles of the spent He-pretreated and spent precarburized 6Mo-1Fe/HZSM-5 catalysts in Figures 12 and 13 respectively. This implies that at high iron loadings the formation of “hard coke” cannot be avoided with pretreatment. Weak, broad peaks are observed in all the fresh precarburized catalysts. 6Mo/ZSM-5 exhibits a peak at around 470°C, while 6Mo-0.2Fe/ZSM-5 shows a peak at around 440°C, and 6Mo-1Fe/ZSM-5 presents two peaks at around 450°C and 540°C. The low temperature peaks can be attributed to the start of the formation of the Mo associated carbon deposits, which are also detected by TGA. Since we observe carbon nanotubes in fresh 6Mo-1Fe/ZSM-5, we can assign the higher temperature peak, at 540°C, to the carbon nanotubes.

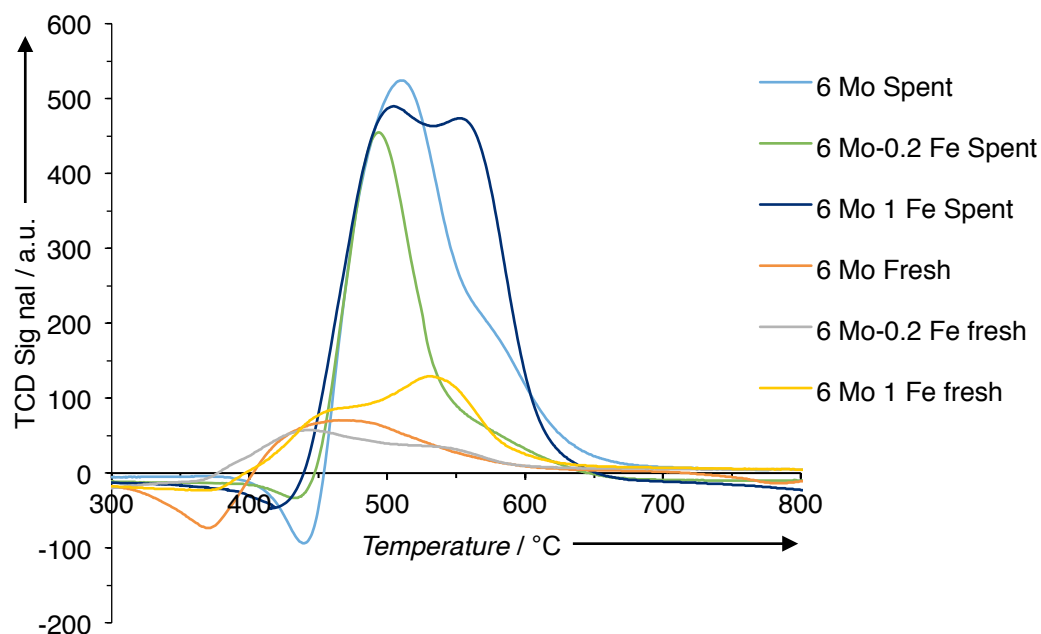


Figure 13. TPO of fresh and spent precarburized catalysts 6Mo/ZSM-5, 6Mo-0.2 Fe/ZSM-5 and 6Mo-1Fe/ZSM-5. (The spent catalysts underwent reaction at 700°C under 91% CH₄/N₂ with a space velocity of 1500 ml/g·hr for 10 hours.)

Discussion

Much research has been dedicated to improving Mo/ZSM-5 catalysts for methane aromatization. Amongst the different techniques, addition of promoters, such as Fe^[25-30], and use of different pretreatment methods have been extensively studied^{[32][33][44][45]}. The results obtained with Fe additive are not conclusive, since different groups obtain different results based on the synthesis method and on the Mo and Fe loadings employed. However, plenty of work shows the possibility of Fe improving the catalytic behavior of the Mo-based catalysts, and it is therefore worth exploring at a deeper level. To the best of our knowledge, no studies have been performed on the effect of the catalyst pretreatment on Fe-modified Mo/ZSM-5 catalysts and it is therefore the focus of the present work.

Previous work has demonstrated that pretreating Mo/ZSM-5 catalysts in a mixture of CH₄+H₂ results in enhanced catalytic behavior, rendering higher yields to benzene and better catalytic stability [32][33]. Since it is agreed that Mo carbides are the active species responsible for the activation of CH₄, it is reasonable to assume that precarburizing the supported Mo oxides must result in improved catalytic behavior. Indeed, in our recent work [46] we have discovered that preparing HZSM-5 supported Mo carbides *ex situ*, and then applying them in methane aromatization reaction drastically improves the catalytic behavior compared to supported Mo oxides, where the active carbide species are formed *in situ* during the reaction induction period. Furthermore, employing higher loadings of Mo carbides (up to 12 wt% Mo) result in higher and more stable benzene yields over long periods of time, compared to oxides with the same Mo loadings. The latter is probably due to the formation of a larger amount of carbide species that are better dispersed in the zeolite channels when they are prepared *ex situ*.

In the present work, we have employed Mo catalysts consisting of 6 wt% Mo supported on ZSM-5, since our previous results on effect of Mo loading (testing in the range of 3-12 wt% Mo) when catalysts were pretreated in He showed the best catalytic behavior with 6 wt% loading of Mo [46]. To test the influence of Fe addition, we have modified our 6Mo/ZSM-5 catalyst with a 0.2wt% Fe (low Fe loading) and a 1wt% Fe loading (higher Fe loading). The choice of overall low Fe loadings is due to previous literature results [28-30] which show that generally when Fe is used as a dopant, lower loadings are more beneficial to catalytic behavior.

The activity results (Figure 1) indicate that adding Fe to 6Mo/ZSM-5 improves catalytic performance regardless of the type of pretreatment that the catalysts are subject to. When catalysts are pretreated in He, an improvement is observed with 0.2 wt% Fe, however, adding 1wt% Fe slightly decreases the benzene yield compared to 6Mo/ZSM-5. This result, which is in line with previous results published in literature [29,30], indicates that for a certain loading of Mo there is an optimum Fe loading that can enhance the catalyst performance, and in our case, for 6wt% Mo, this is 0.2 wt% Fe. Upon precarburizing the same catalysts, there is a general increase in benzene yield compared to the He pretreated samples (in Figure 1, all points corresponding to precarburized samples are higher than He pretreated catalysts), and moreover, addition of both 0.2 and 1 wt% Fe enhances the performance of the 6Mo/ZSM-5 catalyst. More importantly, the catalysts become more stable since the benzene yield drops with a less inclined slope for precarburized 6Mo and 6Mo-1Fe/ZSM-5 compared to their He pretreated counterparts. In the case of 6Mo-0.2Fe/ZSM-5 this catalyst remains stable all the time, with no decrease in benzene yield. Therefore, combining the use of Fe dopant with a reduction + carburization pretreatment results in a catalyst that provides improved yield to benzene with the additional advantage that it overcomes deactivation and remains stable over long periods of time.

To understand how the presence of Fe affects the reactivity of the Mo sites, benzene selectivity versus CH₄ conversion data were represented for all catalysts (Figure 3); the results show that regardless of the type of pretreatment received, the nature of the sites in all three catalysts are different, since different benzene selectivity values are obtained for similar CH₄ conversions. For same values of CH₄ conversion, the benzene selectivities obtained with 0.2 wt% Fe are higher than with 1 wt% Fe. Although the CH₄ conversions remain lower than for 6Mo/ZSM-5, the benzene selectivities are high enough that the benzene yield obtained with 0.2wt% Fe remains higher than in the absence of Fe. The TPR results of the fresh He pretreated samples indicate that the reducibility of the Mo sites changes upon addition of Fe, which could explain the different behavior of these sites in reaction. Specifically, the MoO₂ to Mo reduction peak shifts to slightly

lower temperature for the 6Mo0.2Fe/ZSM-5 sample (760 °C) compared to the 6Mo/ZSM-5 sample (790 °C), making the former more reducible. For the active Mo carbide sites to form in reaction, it is required that the Mo oxide species reduces to Mo⁰, thus, higher reducibility will result in easier formation of Mo carbide phases and consequently better catalytic activity. When 1wt% Fe is added, the peak shifts to higher temperature (800 °C and a shoulder at 850 °C), thus making the sites less reducible, which could explain the lower benzene yields obtained with this catalyst compared to 6Mo/ZSM-5 (open symbols in Figure 1).

Structural characterization of the fresh catalysts was performed to detect metal phases on the ZSM5 support. As expected, for the He pretreated samples, MoO₃ crystalline species are detected by XRD and the peak corresponding to MoO₃ becomes less intense upon adding Fe, probably because Fe interactions with Mo species decrease their crystallinity. No other crystalline Fe, mixed Mo-Fe or Mo-Al phases are detected. Some investigations, have reported that Mo loadings greater than 4 wt.% lead to dealumination, resulting in the formation of Al₂(MoO₄)₃ which was detected using Al-NMR [47][48]. Masiero et al. [29] were able to detect Al₂(MoO₄)₃ in 8 wt%Mo-2 wt%Fe oxides supported on ZSM-5 and 12 wt% Mo-3 wt%Fe supported on ZSM-5 using XRD. However, for the catalysts presented here, no characteristic reflections of Al₂(MoO₄)₃ were observed. Masiero et al. [29] also obtained reflections of Fe₂(MoO₄)₃ at, 24.9°C, 25.7°C and 27.5°C, but no other crystalline species corresponding to mixed Mo-Fe species were detected in our samples. In the case of the precarburized catalysts, no crystalline Mo or Fe species (Mo and/or Fe oxides and carbides) are detected, which indicates that the Mo species are better dispersed in the zeolite structure and channels after reduction + carburization pretreatment. This could explain the better catalytic behavior of the precarburized catalysts. The absence of mixed Mo-Fe crystalline phases is not surprising since we have used very low loadings of Fe compared to the loading of Mo. It is probable that Fe has an influence on the electronic properties of Mo without forming any mixed phases.

In the precarburized catalysts no carbide species are detected by XRD, although we would expect them to have formed after reduction and carburization. Mo carbide speciation is not an easy task, especially at low loadings, since few characterization techniques can detect them directly. Employing XPS and XAS analysis, Wang et al. [49] and Li et al. [50] have respectively been able to show that Mo oxide species convert to Mo carbide species during CH₄ aromatization reaction. Iglesia's group reached similar conclusions by performing in situ XANES experiments [43]. Recently Mo carbide and oxycarbide species were detected by performing operando synchrotron X-Ray measurements [51]. We speculate that these phases are present in our samples in the form of well dispersed small atomic clusters that can be detected by Near Edge X-Ray Absorption techniques and we currently have ongoing experiments addressing this characterization. However, our TGA results can give us an indirect hint on the existence of carbide species in the precarburized samples (Figure 11). The slight weight gain observed during the oxidation of the fresh precarburized catalysts in the 300-400 °C range indicates that carbide species are being oxidized to oxide species. The TGA results also indicate the presence of carbon deposits in the fresh catalysts, which must have been formed during the precarburization treatment. The fact that more carbon deposits are formed in the fresh precarburized 6Mo-1Fe/ZSM-5 catalyst compared to 6Mo-0.2Fe/ZSM-5 can explain its lower stability in reaction.

To better understand the effect of the presence of Fe and of the type of pretreatment on the catalytic stability, we contrasted the characterization results of the fresh catalysts with the spent

catalysts. The XRD patterns of the spent catalysts (both He pretreated and precarburized) show no peaks corresponding to crystalline phases, except the ZSM-5 support. Only in the case of 6Mo-1Fe/ZSM-5 a broad peak which could be assigned to Mo₂C is observed, indicating possible sintering of this species after reaction. This could explain the generally worse catalytic performance of this catalyst compared to the 6Mo-0.2Fe/ZSM-5 catalyst. Analysis of the BET surface areas of fresh and spent catalysts clarifies more the reason for different stability in the catalysts. It is observed that the % drop in surface area between fresh and spent catalysts is larger in the He pretreated samples (~45%) compared to the precarburized samples (29-14%), explaining the higher stability and benzene yields obtained with the latter. Furthermore, TGA analysis of the amount of carbon deposits formed in reaction (Table 3) for the precarburized samples indicates that the amount of carbon deposited for 6Mo-0.2Fe/ZSM-5 (56 mg/g of catalyst) is almost half the amount deposited for 6Mo-1Fe/ZSM5 (106 mg/g of catalyst). Therefore, formation of a lower quantity of carbon deposits explains the lower decrease in surface area and thus the higher stability of the 6Mo-0.2Fe/ZSM-5 catalyst compared to 6Mo-1Fe/ZSM5 and 6Mo/ZSM5. When comparing 6Mo/ZSM-5 and 6Mo-1Fe/ZSM-5 catalysts, we observe that the latter is more stable and presents a smaller % drop in surface area after reaction compared to the former, despite containing more carbon deposits after reaction (69 mg/g of catalyst for 6Mo/ZSM-5 versus 106 mg/g for 6Mo-1Fe/ZSM-5).

The higher stability of precarburized 6Mo-1Fe/ZSM-5 compared to that of 6Mo/ZSM-5 can be justified based on the morphology of the C deposits observed in the SEM images in Figure 10. Carbon nanotubes are observed in the spent 6Mo-1Fe/ZSM-5 catalyst, but they are not detected in absence of Fe. It is known from past work that carbon nanotubes do not reduce surface area due to their hollow structure, and allow diffusivity of reactants and products ^[30], therefore, despite a higher presence of deposits in the spent 6Mo-1Fe/ZSM-5 catalyst compared to 6Mo/ZSM-5, since they are in the form of carbon nanotubes, the reactant molecules still have access to the active sites, and thus the catalysts are capable of yielding benzene over longer periods of time than 6Mo/ZSM-5.

The presence of carbon nanotubes in the catalyst with higher Fe loading (6Mo-1Fe/ZSM-5) is in line with previous research which attributes the formation of carbon nanotubes to the presence of Fe ^{[30][52][53]}. Abdelsayed and coworkers ^[53] observed carbon nanotubes in their Mo-Fe catalysts. Sun and coworkers ^[28] observed formation of carbon nanotubes in both Mo and Mo-Fe catalysts, but they claimed that formation of carbon nanotubes was more extensive in Mo-Fe catalysts. Also, it is interesting to observe that just after precarburization, there was no change in the morphology of 6Mo/ZSM-5 and 6Mo-0.2Fe/ZSM-5, but a small amount of carbon nanotubes was observed in 6Mo-1Fe/ZSM-5, corroborating that increasing the Fe content in the catalyst triggers the formation of carbon nanotubes.

It is important to note that when the catalysts are pretreated in He, carbon nanotubes are observed also in the 6Mo-0.2Fe/ZSM-5 spent catalyst. Therefore, it is probable that precarburization inhibits the formation of carbon nanotubes. Considering that the precarburization treatment consists of careful temperature programmed reduction and carburization of the supported oxides, which is a common method employed to prepare high surface area metal carbides, it is reasonable to assume that this pretreatment can result in a better formation of more dispersed Mo carbide species before reaction, and thus can prevent rapid deposition of deactivating carbon.

Of the catalysts tested, 6Mo-0.2Fe/ZSM-5 presents the highest benzene yields and hardly deactivates with TOS when it is precarburized. Analyzing the SEM image of the spent precarburized 6Mo-0.2Fe/ZSM-5 catalyst indicates no formation of carbon nanotubes, despite the presence of Fe, and the total amount of carbon deposited after reaction (from TGA measurements) is lower than in the cases of 6Mo/ZSM-5 and 6Mo-1Fe/ZSM-5. Additionally, the conversion/selectivity results indicate that the nature of the 6Mo-0.2Fe/ZSM-5 sites are different from those present in 6Mo/ZSM-5 and 6Mo-1Fe/ZSM-5. No mixed Mo-Fe phases are detected by XRD, therefore we speculate that the presence of a small amount of Fe can modify the electronic properties of Mo sites in a way which changes the reaction pathway, leading to an enhancement in the formation of aromatics and fewer carbon deposits. To understand the electronic influence of such a small quantity of Fe on Mo, the structure of the catalysts needs to be further explored employing more advanced characterization techniques such as XPS and X-Ray Absorption.

Conclusions

When Fe is incorporated into Mo/ZSM-5 catalysts, the yields to benzene are enhanced in the methane aromatization reaction. However, there is an optimum Fe loading, since higher loadings can lead to a decline in catalytic behavior. The type of pretreatment also affects the catalysts' performance in reaction, and pretreating by reducing and carburizing results in lower catalyst deactivation and higher benzene yields. Since carbides are thought to be the active sites for methane aromatization, it is probable that during precarburization, a higher quantity and better distribution of these phases are created before reaction, leading to enhanced catalytic properties. The nature of the active sites is different depending on the Fe loading, which is corroborated by TPR measurements, which show that adding a small amount of Fe (0.2 wt%) increases the reducibility of the Mo sites. In the precarburized samples, it is observed that the catalyst with 0.2 wt% Fe loading is the most stable catalyst, which is consistent with its lower carbon content and higher surface area after reaction compared to the catalysts with 0 and 1 wt% Fe.

Experimental Section

Catalyst Preparation

Commercial ZSM-5 (Si/Al=15, Zeolyst International) was used as the support for the catalysts. The commercial ZSM-5 was first calcined at 500°C with ramp rate of 2°C/min for 6 hours to convert the zeolite powder from its ammonium form to its protonated form. Molybdenum oxide was supported on the zeolite using the conventional incipient wetness impregnation method. Ammonium heptamolybdate tetrahydrate (Sigma Aldrich) and ferric nitrate nonahydrate were used as the metal precursors for Mo and Fe respectively. Sequential impregnation method was employed to prepare the mixed Mo-Fe-ZSM-5 catalysts using the above-mentioned precursors. The resulting samples were then dried overnight and calcined in the furnace at 110°C with a ramp rate of 1°C/min and held at this temperature for 2 hours, followed by calcination at 500°C at 1°C/min for 5 hours. The catalysts that were prepared contained 6 wt% Mo and different amounts of Fe (0, 0.2 and 1 wt% Fe) and are respectively designated as 6Mo-ZSM-5, 6Mo-0.2Fe/ZSM-5, and 6Mo-1Fe/ZSM-5.

Catalyst reactivity

The catalysts were tested in a fixed-bed quartz tube reactor with 0.3 g of 250-125 microns sized sample located between two quartz wool plugs. The samples were heated to 700°C with a 1°C temperature ramp, under a different gas flow depending on the chosen pretreatment condition (described in the following section); after temperature equilibration at 700°C was achieved, reaction conditions were applied by flowing 91% CH₄/N₂ into the reactor at atmospheric pressure and at a space velocity of 1500 ml/g·h. With nitrogen as an internal standard, the products leaving the reactor were analyzed using an online gas chromatograph equipped with flame ionization detector and thermal conductivity detector (Shimadzu).

Pretreatment conditions

Two pretreatment methods were tested: (a) heating the catalyst to 700°C under He flow (b) reducing the catalyst with a CH₄/H₂ (1:9, v/v) mixture until 700°C, and then carburizing for 10 mins under pure CH₄ at 700°C. We will refer to this second pretreatment method as “precarburization”.

Catalyst Characterization

Both fresh and spent catalysts were characterized by the following characterization methods.

Brunauer-Emmett-Teller (BET) Surface Area

Textural characteristics of the samples was determined by adsorption of nitrogen at -196°C using Quantachrome Autosorb IQ. The sample was outgassed at 350°C for a minimum of 2 hours and then cooled to -196°C. Adsorption isotherms were then recorded as a function of relative pressure and specific volume of nitrogen adsorbed at Standard Temperature and Pressure (STP). The surface area of the samples was determined using the BET method.

Scanning electron Microscopy (SEM)

The surface morphology of the samples was assessed using Hitachi-H-800 scanning electron microscope. Fresh catalyst samples were analyzed at 8-10kV, while the spent samples were analyzed at 8kV.

X-Ray diffraction patterns of the catalyst (XRD)

X-Ray diffraction patterns of the catalyst were obtained using Rigaku Ultima III PXRD with CuK α radiation at 40kV and 20mA. The data was recorded at 2 θ between 5° to 60° at a scan speed of 0.25°/min.

Temperature Programmed Oxidation (TPO)

TPO was carried out on fresh catalysts using Quantachrome-Autosorb IQ. The sample was heated to 500°C at 20°C /min under He flow, and held for 30 mins, after which the sample was brought back to room temperature. The gas was switched from He to 9.9% O₂/He, and the sample was heated to 800°C at 10°C /min. The data was recorded using in-built TCD.

Temperature Programmed Reduction (TPR)

TPR was carried out on fresh catalysts before pretreatment using Quantachrome-autosorb iq. In order to maintain consistency, 0.0700 gms of the sample was weighed out. The procedure adopted was similar to TPO, where the sample was heated to 500°C at 20°C/min under He flow, and held for 30 mins, after which the sample was brought back to room temperature. The gas was switched from He to 5%H₂/He, and the sample was heated to 1000°C at 10°C/min. The data was recorded using an in-built TCD.

Thermogravimetric analysis (TGA)

TGA was performed on the spent catalysts using METTLER TGA/SDTA851e. 0.015 g of sample was heated to 1000 °C at 10 °C/min under airflow of 50 ml/min. The amount of coke in the spent catalyst was calculated as follows: ^[54]

$$\text{Coke amount (mg/g. cat)} = \frac{M_2 - M_3}{M_3} \times 1000$$

Where M₂ denotes the weight percent of the coked catalyst before burning-off the coke, and M₃ denotes the weight percent of the coked catalyst after burning off the coke.

Acknowledgements

The authors acknowledge the financial support received from Texas Tech University. The authors would like to thank Dr. Daniel Unruh from the Department of Chemistry and Biochemistry for his help in acquiring the XRD patterns.

Keywords: methane aromatization; 6wt% Mo/HZSM-5; Fe additive; catalytic activity; carbon deposits.

References)

-
- [1] M. Ruitenbeek, B. M. Weckhuysen, *Angew. Chem. Int. Ed.* **2015**, *46(1)*, 11137-11139.
 - [2] K. Dutta, L. Li, P. Gupta, D. P. Gutierrez, J. Kopyscinski, *Catal. Commun.* **2018**, *106*, 16-19.
 - [3] S. Ma, X. Guo, L. Zhao, S. Scott, X. Bao, *J. Energy Chem.* **2013**, *22(1)*, 1-20.
 - [4] L. Wang, L. Tao, M. Xie, G. Xu, J. Huang, Y. Xu, *Catal. Lett.* **1993**, *21(1-2)*, 35-41.

-
- [5] D. Wang, J. H. Lunsford, M. P. Rosynek, *J. Catal.* **1997**, *169*(1), 347-358.
- [6] S. Liu, L. Wang, R. Ohnishi, M. Ichikawa, *J. Catal.* **1999**, *181*(2), 175-188.
- [7] Y. Xu, S. Liu, X. Guo, L. Wang, M. Xie, *Catal. Lett.* **1995**, *30*(1-4), 135-149.
- [8] Y. Xu, Y. Shu, S. Liu, J. Huang, X. Guo, *Catal. Lett.* **1995**, *35*(3-4), 233-243.
- [9] E. V. Matus. PhD thesis, Boreskov Institute of Catalysis, Novosibirsk, Russia, 2007.
- [10] W. Ding, G.D. Meitzner, E. Iglesia, *J. Catal.* **2002**, *206*(1), 14-22.
- [11] S. Wong, Y. Xu, W. Liu, L. Wang, X. Guo, *Appl. Catal. A: Gen.* **1996**, *136*(1), 7-17.
- [12] Y. Shu, H. Ma, R. Ohnishi, M. Ichikawa, *Chem. Commun.* **2002**, *1*, 86-87.
- [13] D. Ma, Y. Shu, X. Han, X. Liu, Y. Xu, X. Bao, *J. Phys. Chem. B* **2001**, *105*(9), 1786-1793.
- [14] Y. Shu, D. Ma, X. Liu, X. Han, Y. Xu, X. Bao, *J. Phys. Chem. B.* **2000**, *104*(34), 8245-8249.
- [15] A. Martínez, E. Peris, G. Sastre, *Cat. Today* **2005**, *107-108*, 676-684.
- [16] C.H. Tempelman, V.O. Rodrigues, E.R. Eck, P.C. Magusin; E.J. Hensen, *Micropor. Mesopor. Mat.* **2015**, *203*, 259-273.
- [17] Y. Shu, R. Ohnishi, M. Ichikawa, *J. Catal.* **2002**, *206*(1), 134-142.
- [18] H. Lacheen, E. Iglesia, *J. Catal.* **2005**, *230*(1), 173-185.
- [19] L. Wang, Y. Xu, S. Wong, W. Cui, X. Guo, *Appl. Catal. A: Gen.* **1997**, *152*(2), 173-182.
- [20] R. Kojima, S. Kikuchi, H. Ma, J. Bai, M. Ichikawa, *Catal. Lett.* **2006**, *110*(1-2), 15-20.
- [21] S. Li, C. Zhang, Q. Kan, D. Wang, T. Wu, L. Lin, *Appl. Catal. A: Gen.* **1999**, *187*(2), 199-206.
- [22] S. Liu, L. Wang, R. Ohnishi, M. Ichikawa, *J. Catal.* **1999**, *181*(2), 175-188.
- [23] S. Burns, J. Hargreaves, P. Pal, K. Parida, S. Parija, *Catal. Today* **2006**, *114*(4), 383-387.
- [24] M. Ngobeni, A. Carley, M. Scurrell, C. Nicolaidis, *J. Molec. Catal. A: Chem.* **2009**, *305*(1-2), 40-46.

- [25] A.K. Aboul-Gheit, M.S. El-Masry, A.E. Awadallah, *Fuel Process. Technol.* **2012**, *102*, 24-29.
- [26] A.K. Aboul-Gheit, A.E. Awadallah, S.M. El-Kossy, A.H. Mahmoud, *J. Nat. Gas Chem.* **2008**, *17(4)*, 337-343.
- [27] P. Tan, *J. Catal.* **2016**, *338*, 21-29.
- [28] K. Sun, W. Gong, K. Gasem, H. Adidharma, M. Fan, R. Chen, R. *Ind. Eng. Chem. Res.* **2017**, *56(40)*, 11398-11412.
- [29] S.S. Masiero, N.R. Marcilio, O.W. Perez-Lopez, *Catal. Lett.* **2009**, *131(1-2)*, 194-202.
- [30] Y. Xu, J. Wang, Y. Suzuki, Z. Zhang, *Catal. Today* **2012**, *185(1)*, 41-46.
- [31] T. Kubota, N. Oshima, Y. Nakahara, M. Yanagimoto, Y. Okamoto, *J. Japan Petrol. Instit.*, **2006** *49(3)*, 127-133
- [32] C.H. Tempelman, E.J. Hensen, *Appl. Catal. B: Environ.* **2015**, *176-177*, 731-739.
- [33] P. Tan, *Catal. Commun.* **2018**, *103*, 101-104.
- [34] B. Li, S. Li, N. Li, H. Chen, W. Zhang, X. Bao, B. Lin, *Micropor. Mesopor. Mater.* **2006**, *88(1-3)*, 244-253.
- [35] S. Rajagopal, H.J. Marini, J.A. Marzari, R. Miranda, *J. Catal.* **1994**, *147(2)*, 417-428.
- [36] P. Arnoldy, J.C. Jonge, J.A. Moulijn, *J. Phys. Chem.* **1985**, *89(21)*, 4517-4526.
- [37] A. Martínez, E. Peris, *Appl. Catal. A: Gen.* **2016**, *515*, 32-44.
- [38] H.-Y. Lin, Y.-W. Chen, C. Li, *Thermochim. Acta.* **2003**, *400*, 61-67.
- [39] S. Jiang, H. Zhang, Y. Yan, X. Zhang, *RSC Adv.* **2015**, *5(51)*, 41269-41277.
- [40] B. Liu, L. France, C. Wu, Z. Jiang, V.L. Kuznetsov, H.A. Al-Megren, P.P. Edwards, *Chem. Sci.* **2015**, *6(9)*, 5152-5163.
- [41] H. Liu, T. Li, B. Tian, Y. Xu *Appl. Catal. A: Gen.* **2001**, *213(1)*, 103-112.
- [42] Y. Li, L. Liu, X. Huang, X. Liu, W. Shen, Y. Xu, X. Bao, *Catal. Commun.* **2007**, *8(11)*, 1567-1572.
- [43] W. Ding, S. Li, G.D. Meitzner, E. Iglesia, *J. Phys. Chem. B* **2001**, *105(2)*, 506-513.

-
- [44] Y. Song, Y. Xu, Y. Suzuki, H. Nakagome, Z.-G. Zhang, *Appl. Catal. A: Gen.* **2014**, *482*, 387-396.
- [45] Y. Song, Y. Xu, H. Nakagome, X. Ma, Z.-G. Zhang, *J. Catal.* **2015**, *330*, 261-272.
- [46] M. Rahman, A. Sridhar, S.J. Khatib, *Appl. Catal. A: Gen.* (submitted).
- [47] R.W. Borry, Y.H. Kim, A. Huffsmith, J.A. Reimer, E. Iglesia, *J. Phys. Chem. B* **1999**, *103(28)*, 5787-5796.
- [48] W. Zhang, D. Ma, X. Han, X. Liu, X. Bao, X. Guo, X. Wang, *J. Catal.* **1999**, *188(2)*, 393-402.
- [49] L. Wang, L. Tao, M. Xie, G. Xu, J. Huang, Y. Xu, *Y. Catal. Lett.*, **1993**, *21*, 35-41.
- [50] W. Li, G.D. Meitzner, Y.H. Kim, R.W. Borry, E. Iglesia, *Stud. Surf. Sci. Catal.* **2000**, *130*, 3621-3626.
- [51] I. Lezcano-Gonzalez, R. Oord, M. Rovezzi, P. Glatzel, S.W. Botchway, B.M. Weckhuysen, A.M. Beale, *Angew. Chem. Int. Ed.* **2016**, *55*, 5215-5219.
- [52] Y. Xu, Y. Suzuki, Z. Zhang, *Appl. Catal. A: Gen.* **2013**, *452*, 105-116.
- [53] V. Abdelsayed, D. Shekhawat, M.W. Smith, *Fuel*, **2015**, *139*, 401-410.
- [54] H. Liu, T. Li, B. Tian, Y. Xu, *Appl. Catal. A: Gen.* **2001**, *213(1)*, 103-112.